HHS Public Access

Author manuscript

*Angew Chem Int Ed Engl*. Author manuscript; available in PMC 2018 September 11.

Published in final edited form as:

*Angew Chem Int Ed Engl*. 2017 September 11; 56(38): 11404–11408. doi:10.1002/anie.201704649.

# Fluorous Phase-Directed Peptide Assembly Affords Nano-Peptisomes Capable of Ultrasound-Triggered Cellular Delivery

**Scott H. Medina**,
Department of Biomedical Engineering, The Pennsylvania State University, 223 Hallowell, University Park PA, 16802 (USA)

**Megan S. Michie**,
Chemical Biology Laboratory, National Cancer Institute, National Institutes of Health, 376 Boyle Street, Frederick MD, 21702-1201 (USA)

**Stephen E. Miller**,
Chemical Biology Laboratory, National Cancer Institute, National Institutes of Health, 376 Boyle Street, Frederick MD, 21702-1201 (USA)

**Martin J. Schnermann**, and
Chemical Biology Laboratory, National Cancer Institute, National Institutes of Health, 376 Boyle Street, Frederick MD, 21702-1201 (USA)

**Joel P. Schneider**
Chemical Biology Laboratory, National Cancer Institute, National Institutes of Health, 376 Boyle Street, Frederick MD, 21702-1201 (USA)

## Abstract

Here, we report the design, synthesis and efficacy of a new class of ultrasound (US)-sensitive self-assembled peptide-based nanoparticle. Peptisomes are prepared via templated assembly of a *de novo* designed peptide at the interface of fluorinated nanodroplets. Utilizing peptide assembly allows for facile particle synthesis, direct incorporation of bioactive sequences displayed from the particle corona, and the ability to easily encapsulate biologics during particle preparation using a mild solvent exchange procedure. Further, nano-peptisome size can be precisely controlled by simply modulating the starting peptide and fluorinated solvent concentrations during synthesis. Biomolecular cargo encapsulated within the particle core can be directly delivered to the cytoplasm of cells upon US-mediated rupture of the carrier. Thus, nano-peptisomes represent a novel class of US-activated carriers that can shuttle cell-impermeable biomacromolecules into cells with spatial and temporal precision.

## COMMUNICATION

Correspondence to: Scott H. Medina; Joel P. Schneider.

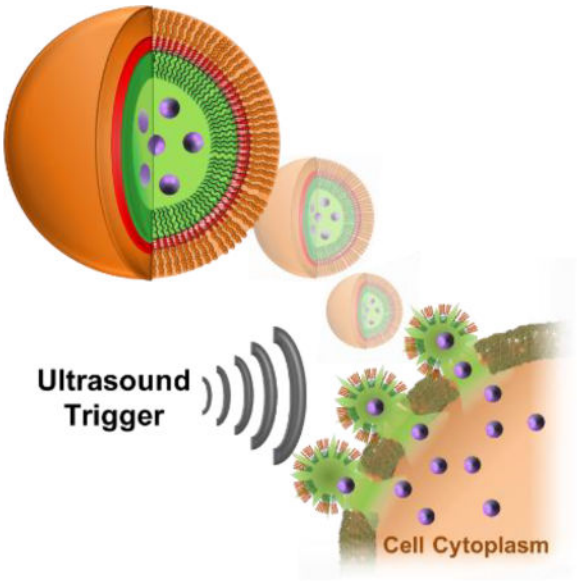


**Burst your bubble:** The templated assembly of a *de novo* designed peptide at the interface of fluorous nanodroplets affords ultrasound-sensitive nano-peptisomes. Acoustic rupture of the carrier at the surface of cells leads to direct intracellular delivery of encapsulated membrane-impermeable biomolecular cargo with spatial and temporal precision.

## Keywords

peptides; self-assembly; nanostructures; ultrasound; drug delivery

Peptide assembly is a spontaneous self-sorting process that can lead to the formation of dynamic nanostructures. Often, the architecture and behavior of the final assembly can be controlled by modulating the physicochemical properties of the building blocks, environmental conditions or assembly kinetics.[1] This has produced a wide variety of ordered states, including sheets,[2] fibrils,[3] and tubes,[3h, 4] which are playing increasingly important roles in the formation of biomaterials and biomedical devices. Here, we report the development of nano-peptisomes prepared through the templated assembly of peptide amphiphiles at a fluorous-liquid interface (Figure 1). Nano-peptisomes contain a perfluorocarbon liquid interior that allows for activation of the particle upon application of ultrasound (US). Acoustic vaporization of the fluorous liquid leads to the formation of a gaseous core that ultimately swells and ruptures the nano-peptisome. Subsequent bubble cavitation produces a high intensity pressure wave that, if generated at the surface of a cell, transiently permeabilizes the plasma membrane,[5] and simultaneously ejects encapsulated molecular cargo. Thus, US-sensitive nano-peptisomes represent a spatially and temporally controlled delivery modality that, as will be shown, can shuttle loaded biomacromolecules directly into the cytoplasm of cells, thereby avoiding endosomal uptake and degradation of the bioactive payload.

Key to the assembly of these nano-peptisomes is the *de novo* designed peptide $F_FF_FF_F$GGGCCGGKGRGD-$NH_2$, capable of assembling at the surface of a perfluoro-*n*-

pentane (PFP) droplet. This sequence contains three pentafluoro-phenylalanine ($F_F$) residues at its N-terminus, which promotes interpolation and assembly of the peptide at the PFP-liquid interface. C-terminal to this fluorous domain is a cysteine containing motif (GGGCCGG) designed to undergo disulfide cross-linking to stabilize the peptide corona after templated assembly. Incorporation of a bioactive hydrophilic sequence at the peptide's C-terminus ultimately leads to its multivalent display at the surface of the assembled particle. In this first design, we include the sequence KGRGD to enable cell-surface localization of the nanoparticle mediated by binding of RGD with extracellular integrins.[6] Gratifyingly, despite inclusion of highly fluorinated residues, this sequence could be chemically synthesized in high yield and purity using standard solid-phase techniques (Supporting Figure 1).

To form nano-peptisomes, we utilized a solvent-exchange procedure in which cold water is slowly added to an organic emulsion of peptide and PFP, ultimately leading to spontaneous assembly of the peptide at the surface of PFP nanodroplets. Importantly, this mild procedure eliminates the need for aggressive synthetic methods commonly used to prepare stimuli-responsive particles,[7] which can lead to degradation of the encapsulated cargo. Subsequent dialysis against 2.5% DMSO in water removed unincorporated peptide, and promoted disulfide cross-linking of cysteine residues in the nanodroplet corona. Cross-linked nano-peptisomes remained stable for multiple weeks when stored at room temperature in water (Supporting Figure 2).

Interestingly, we found that the size of nano-peptisomes could be precisely controlled between 300 – 1200 nm, as a function of peptide and PFP feed ratio (Figure 2a and Table 1). Dynamic light scattering performed on pure PFP emulsions indicates this may be due, in part, to different sizes of PFP droplets formed in the starting emulsion (Supporting Figure 3). At any rate, the ability to control the hydrodynamic radii of the particles is critically important for delivery applications, as this parameter is inversely correlated with passive tissue distribution,[8] and directly proportional to the US magnitude required for droplet cavitation.[9]

We next evaluated the influence of temperature on nano-peptisome size through direct visualization of particles in solution using differential interference contrast (DIC) confocal microscopy (Figure 2b), as well as dynamic light scattering analysis (Supporting Figure 4). Results show that nano-peptisomes with a diameter <750 nm at 25°C were able to maintain their size when heated to physiologic temperature, a vital requirement for acoustic droplet vaporization *in vitro* and *in vivo*.[10] Exceeding this size threshold led to premature PFP vaporization (bp = 29°C) and converted the nanodroplets into gaseous microbubbles at 37°C, as evident by the massive increase in diameter for the purple, green and orange formulations. This influence of particle size on the vaporization temperature of PFP is due to the inverse relationship between internal pressure and droplet dimension, as described by the Laplace pressure equation (1):

$$P_{\mathrm{in}}=\frac{2\sigma}{R_H}+P_{\mathrm{atm}} \quad (1)$$

where $P_{in}$ and $P_{atm}$ are the internal droplet pressure and atmospheric pressure, respectively, $\sigma$ is the interfacial surface tension and $R_H$ represents the hydrodynamic droplet radii. Here, decreasing the droplet size leads to an increase in the pressure exerted on the PFP core, ultimately keeping the fluorous liquid in a superheated state well above its bulk boiling point of 29°C. We can define the influence of vapor pressure on the temperature of the PFP solvent using the Antoine vapor equation (2):

$$\mathrm{T}=\frac{B}{A-\log_{10}\mathrm{P}}-C \quad (2)$$

in which T and P represent temperature and pressure, respectively, while A, B and C are equation parameters empirically determined for PFP.[11] Combining the Laplace pressure (1) and Antoine vapour (2) equations provides a single expression describing the temperature at which the vapour pressure of the core is equal to the internal droplet pressure ($T_{vap}$), ultimately causing thermal droplet vaporization (3):

$$T_{\mathrm{vap}}=\frac{B}{A-\log_{10}\left(\frac{2\sigma}{R_H}+P_{\mathrm{atm}}\right)}-C \quad (3)$$

Using this equation, the relationship between $T_{vap}$ and droplet size can be modelled using reported surface tension values for PFP emulsions formulated with either BSA (0.033 N/m), the amphiphilic polymer PEO-PLA (0.027 N/m), or the cationic surfactant cetrimonium bromide (CTAB; 0.013 N/m) (Supporting Figure 5).[12] Of note, the PFP-CTAB formulation most closely resembles the nano-peptisomes reported here, in which our cationic amphiphilic sequence acts as the surfactant. Results from the model show that, at a surface tension of 0.013 N/m, the vaporization point of the PFP core is expected to be >37°C when particles are <800 nm in size, a finding that closely matches the experimental threshold identified for our PFP-peptide emulsions. This suggests that the US energy required to thermally vaporize the nano-peptisome core could be carefully controlled by modulating the droplet size, as well as changing the interfacial surface tension through tuning the amphiphilic character of the assembling peptide.

Next, we performed a series of experiments to test the stability of nano-peptisomes in physiologic environments, and evaluate their US-mediated delivery potential. For these studies we selected formulation #5 (blue, Table 1) as it remains a droplet at 37°C, and is predicted to have a core $T_{vap}$ slightly higher than physiologic temperature (~40°C). This should, in theory, permit low intensities of US to be used to impart the additional thermal energy necessary for particle vaporization, thereby minimizing potential physical damage to cells and cargo during insonation. At any rate, the stability of nano-peptisomes was first evaluated by subjecting a buffered solution of the nanodroplets to repeated thermocycling, during which dynamic light scattering was used to monitor particle integrity (Figure 3a). Results show that nano-peptisomes not only remained intact under these conditions, but showed little change in overall droplet size.

Conversely, formulation #1 (orange, Table 1) spontaneously vaporized at 37°C to form gaseous microbubbles, which then condensed back to their original size when cooled to room temperature (Figure 3b). The stability of formulation #5 is likely endeared through the disulfide cross-links that are formed between cysteines of adjacent peptides in the nano-peptisome corona. To investigate this possibility, we assessed the propensity of the cysteine resides to undergo oxidation by measuring the rate of disulfide bond formation within freshly prepared nano-peptisomes (Figure 3b, Supporting Figure 6). Results from three independent samples showed that approximately 60% of the available thiols were cross-linked after 1 hour, with a maximum disulfide content of 80% achieved after 24 hours. Control experiments on freshly prepared nano-peptisomes suspended in pure water, without the DMSO oxidizing agent, showed poor cross-linking (~20%) and loss of particle integrity 1 hour after their assembly (Supporting Figure 7).

To assess the delivery potential of nano-peptisomes we loaded fluorescently-labelled phalloidin, a cell-impermeable cyclic peptide that binds to intracellular filamentous actin, into the fluorous core of the particle and monitored its US-mediated transport into cells. Here, encapsulation of this model biomacromolecule was achieved simply by suspending it in the PFP solvent employed for templated assembly of the nano-peptisome carrier. UV spectroscopy performed on nano-peptisomes containing the fluorescently-labelled cargo indicated an encapsulation efficiency of 81%, and an overall loading of $2.3\times10^6$ phalloidin per particle. Particle sizing performed on nano-peptisomes also confirmed the carrier remains stable under the physiologic conditions employed for delivery studies (Supporting Figure 8).

Using flow cytometry, we measured the intracellular fluorescence of A549 lung carcinoma cells following US-mediated phalloidin delivery from nano-peptisomes, varying both the intensity of the acoustic signal and the pulse ratio (duty cycle; DC). Results in Figure 4a show that, in the absence of the US trigger, nano-peptisomes did not effectively deliver the encapsulated fluorescent cargo into cells (see data at 0.0 US intensity for both 10% and 20% DC, where intracellular fluorescence is near zero). However, at US intensities >0 $W/cm^2$ intracellular delivery of phalloidin increased as a function of increasing intensity for both DCs tested. Importantly, cells treated under these conditions of US remained viable and proliferative (Supporting Figure 9). As a control, we also subjected cells to insonation in the presence of unencapsulated phalloidin and PFP, to test the possibility that mechanical permeabilization of cells by US may be responsible for uptake of the fluorescently-labelled biomacromolecule. However, under these conditions no significant increase in intracellular fluorescence was observed across all tested US intensities (Supporting Figure 10).

Fluorescent microscopy performed on live cells after US-mediated delivery of labelled phalloidin confirmed that the cargo was transported into the cytoplasm and remained bioactive, as indicated by its ability to bind to intracellular actin filaments (Figure 4b and Supporting Figure 11; phalloidin visualized as green fluorescence). Importantly, phalloidin was only delivered to the circular area of the cell monolayer exposed to US, showing high spatial resolution over cargo release. Note, the cells outside of the US insonated area (nuclei appear blue) show no intracellular green fluorescence. Further, co-staining treated cells with fluorescently-labelled transferrin, an endosomal marker, showed limited co-localization with

phalloidin fluorescence (Figure 4c). This suggests that biomacromolecules delivered from nano-peptisomes are directly shuttled to the cell cytoplasm and thereby avoid endosomal sequestration. Finally, cell-surface targeting of nano-peptisomes was evaluated by comparing the intracellular fluorescence of cells treated with RGD-containing nano-peptisomes, loaded with labelled phalloidin, versus similar formulations prepared with the non-targeting control sequence RGE (Figure 4c). Results show that RGD-targeted carriers delivered roughly three times the amount of fluorescently-labelled phalloidin into cells compared to the RGE control. Although a moderate increase in cellular fluorescence was observed between untreated cells and those incubated with the non-targeted RGE particles, this is most likely due to non-specific electrostatic interactions between the cationic particle corona and the anionic cellular membrane. Collectively, these studies support our assertion that US-mediated rupture of nano-peptisomes at the plasma membrane can directly deliver encapsulated bioactive macromolecules into the cytoplasm of cells.

In sum, we have developed a new class of peptide-based nanodroplets capable of ultrasound-mediated delivery of membrane-impermeable cargo into cells. Nano-peptisomes are prepared via the *de novo* designed peptide $F_FF_FF_F$GGGCCGGKGRGD-$NH_2$, which efficiently assembles at the surface of organofluorine droplets, and undergoes cysteine-mediated cross-linking to stabilize the final nano-structure. Biomolecular cargo can be readily encapsulated within the nano-peptisome carrier during the assembly process. Cell binding of the nano-peptisomes, followed by acoustic vaporization, ultimately delivers the cargo into cells. Although not demonstrated in this initial report, gaseous microbubbles generated during vaporization of nano-peptisomes may also function as an US contrast agent to allow for imaging and guidance of the delivery modality in real-time.[10b] Thus, nano-peptisomes represent a potential theranostic system with broad applications in drug delivery and biomedical imaging.

## Supplementary Material

Refer to Web version on PubMed Central for supplementary material.

## Acknowledgments

This work was supported by funds provided by Penn State Biomedical Engineering laboratory startup to S.H.M, as well as the NCI Director's Innovation Award and the Intramural Research Program of the National Cancer Institute, National Institutes of Health.

## References

1. Cui H, Webber MJ, Stupp SI. Pept. Sci. 2010; 94:1–18.
2. a) Jang H-S, Lee J-H, Park Y-S, Kim Y-O, Park J, Yang T-Y, Jin K, Lee J, Park S, You JM. Nat. Comm. 2014; 5b) Jiang T, Vail OA, Jiang Z, Zuo X, Conticello VP. J. Am. Chem. Soc. 2015; 137:7793–7802. [PubMed: 26021882] c) Xu F, Khan IJ, McGuinness K, Parmar AS, Silva T, Murthy NS, Nanda V. J. Am. Chem. Soc. 2013; 135:18762–18765. [PubMed: 24283407]
3. a) Amit M, Appel S, Cohen R, Cheng G, Hamley IW, Ashkenasy N. Adv. Funct. Mater. 2014; 24:5873–5880.b) Fukunaga K, Tsutsumi H, Mihara H. Pept. Sci. 2013; 100:731–737.c) Hudalla GA, Sun T, Gasiorowski JZ, Han H, Tian YF, Chong AS, Collier JH. Nat. Mater. 2014; 13:829. [PubMed: 24930032] d) King PJ, Saiani A, Bichenkova EV, Miller AF. Chem. Commun. 2016; 52:6697–6700.e) Kumar VA, Shi S, Wang BK, Li I-C, Jalan AA, Sarkar B, Wickremasinghe NC,

Hartgerink JD. J. Am. Chem. Soc. 2015; 137:4823–4830. [PubMed: 25831137] f) Lin Y-A, Ou Y-C, Cheetham AG, Cui H. Biomacromolecules. 2014; 15:1419–1427. [PubMed: 24611531] g) Luo Z, Wang S, Zhang S. Biomaterials. 2011; 32:2013–2020. [PubMed: 21167593] h) Micklitsch CM, Medina SH, Yucel T, Nagy-Smith KJ, Pochan DJ, Schneider JP. Macromolecules. 2015; 48:1281–1288.

4. a) Ashkenasy N, Horne WS, Ghadiri MR. Small. 2006; 2:99–102. [PubMed: 17193563] b) Li S, Mehta AK, Sidorov AN, Orlando TM, Jiang Z, Anthony NR, Lynn DG. J. Am. Chem. Soc. 2016; 138:3579–3586. [PubMed: 26942690] c) Thomas F, Burgess NC, Thomson AR, Woolfson DN. Angew. Chem. 2016; 128:999–1003.
5. a) Prentice P, Cuschieri A, Dholakia K, Prausnitz M, Campbell P. Nat. Phys. 2005; 1:107–110.b) Deng CX, Sieling F, Pan H, Cui J. Ultrasound Med. Biol. 30:519–526.c) Mehier-Humbert S, Bettinger T, Yan F, Guy RH. J. Controlled Release. 2005; 104:213–222.d) Lee NG, Berry JL, Lee TC, Wang AT, Honowitz S, Murphree AL, Varshney N, Hinton DR, Fawzi AA. Invest. Ophthalmol. Visual Sci. 2011; 52:3868–3873. [PubMed: 21273549]
6. Ruoslahti E. Annu. Rev. Cell Dev. Biol. 1996; 12:697–715. [PubMed: 8970741]
7. Mura S, Nicolas J, Couvreur P. Nat. Mater. 2013; 12:991–1003. [PubMed: 24150417]
8. a) Albanese A, Tang PS, Chan WC. Annu. Rev. Biomed. Eng. 2012; 14:1–16. [PubMed: 22524388] b) Maeda H. J. Controlled Release. 2012; 164:138–144.c) Prabhakar U, Maeda H, Jain RK, Sevick-Muraca EM, Zamboni W, Farokhzad OC, Barry ST, Gabizon A, Grodzinski P, Blakey DC. Cancer Res. 2013; 73:2412–2417. [PubMed: 23423979]
9. a) Martin KH, Dayton PA. Wiley Interdiscip. Rev.: Nanomed. Nanobiotechnol. 2013; 5:329–345. [PubMed: 23504911] b) De Gennes, P-G., Brochard-Wyart, F., Quéré, D. Capillarity and wetting phenomena: drops, bubbles, pearls, waves. Springer Science & Business Media; 2013.
10. a) Shpak O, Verweij M, Vos HJ, de Jong N, Lohse D, Versluis M. Proc. Natl. Acad. Sci. 2014; 111:1697–1702. [PubMed: 24449879] b) Kripfgans OD, Fowlkes JB, Miller DL, Eldevik OP, Carson PL. Ultrasound Med. Biol. 2000; 26:1177–1189. [PubMed: 11053753] c) Giesecke T, Hynynen K. Ultrasound Med. Biol. 2003; 29:1359–1365. [PubMed: 14553814]
11. Barber EJ, Cady GH. J. Phys. Chem. 1956; 60:504–505.
12. Kandadai MA, Mohan P, Lin G, Butterfield A, Skliar M, Magda JJ. Langmuir. 2010; 26:4655–4660. [PubMed: 20218695]

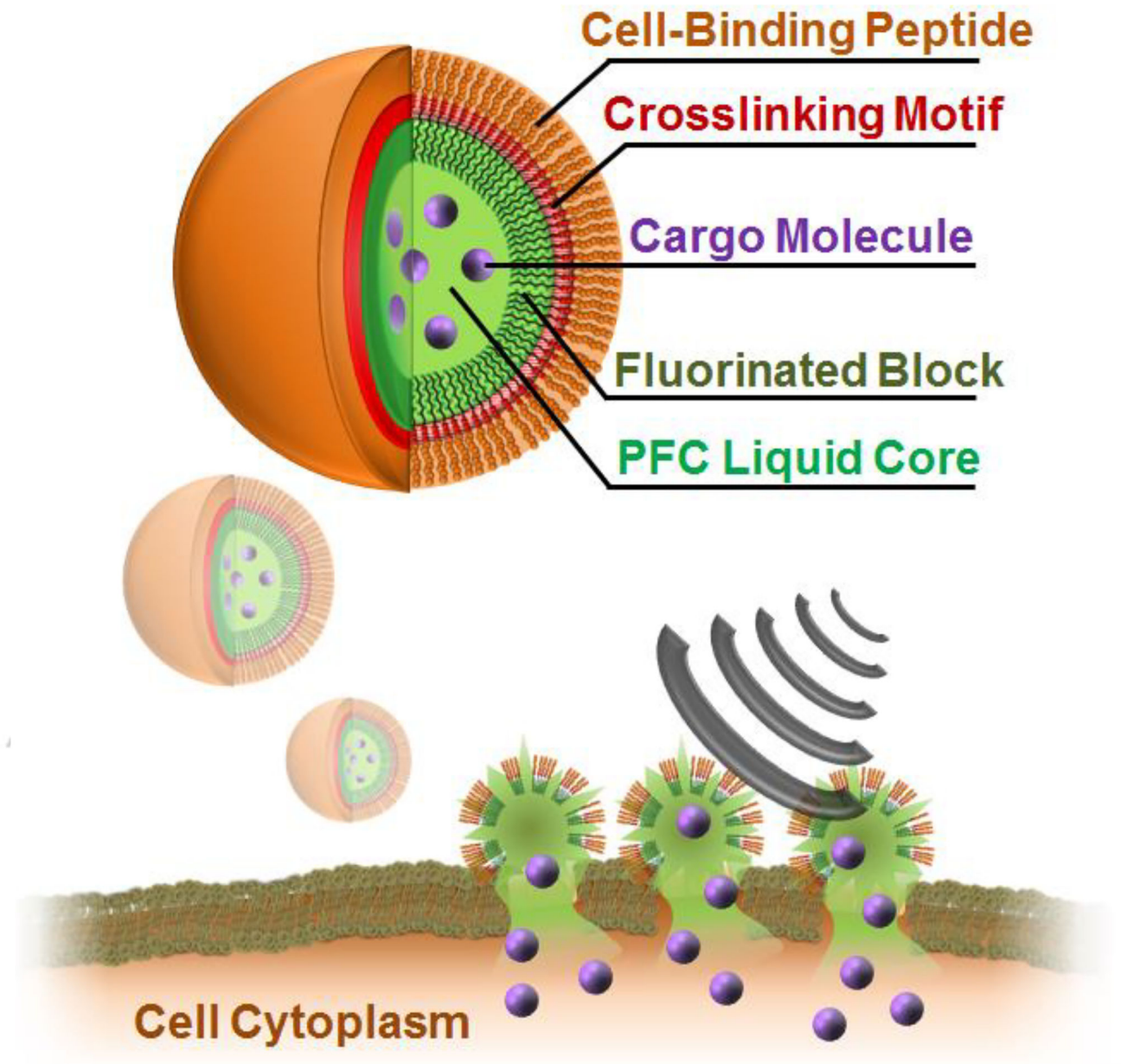


**Figure 1.**

Design and delivery mechanism of nano-peptisomes. Peptisomes are formed from an amphiphilic peptide containing a hydrophilic cell-binding sequence (orange) and a poly-cysteine cross-linking core (red). A C-terminal fluorinated amino acid block (dark green) promotes peptide assembly at the surface of the perfluorocarbon (PFC) liquid core (light green), containing the bioactive cargo (purple). Following binding of nano-peptisomes to the surface of cells, US-mediated vaporization of the fluorous liquid interior leads to a cavitation event that permeabilizes the cell membrane and delivers the loaded cargo into the cytoplasm.

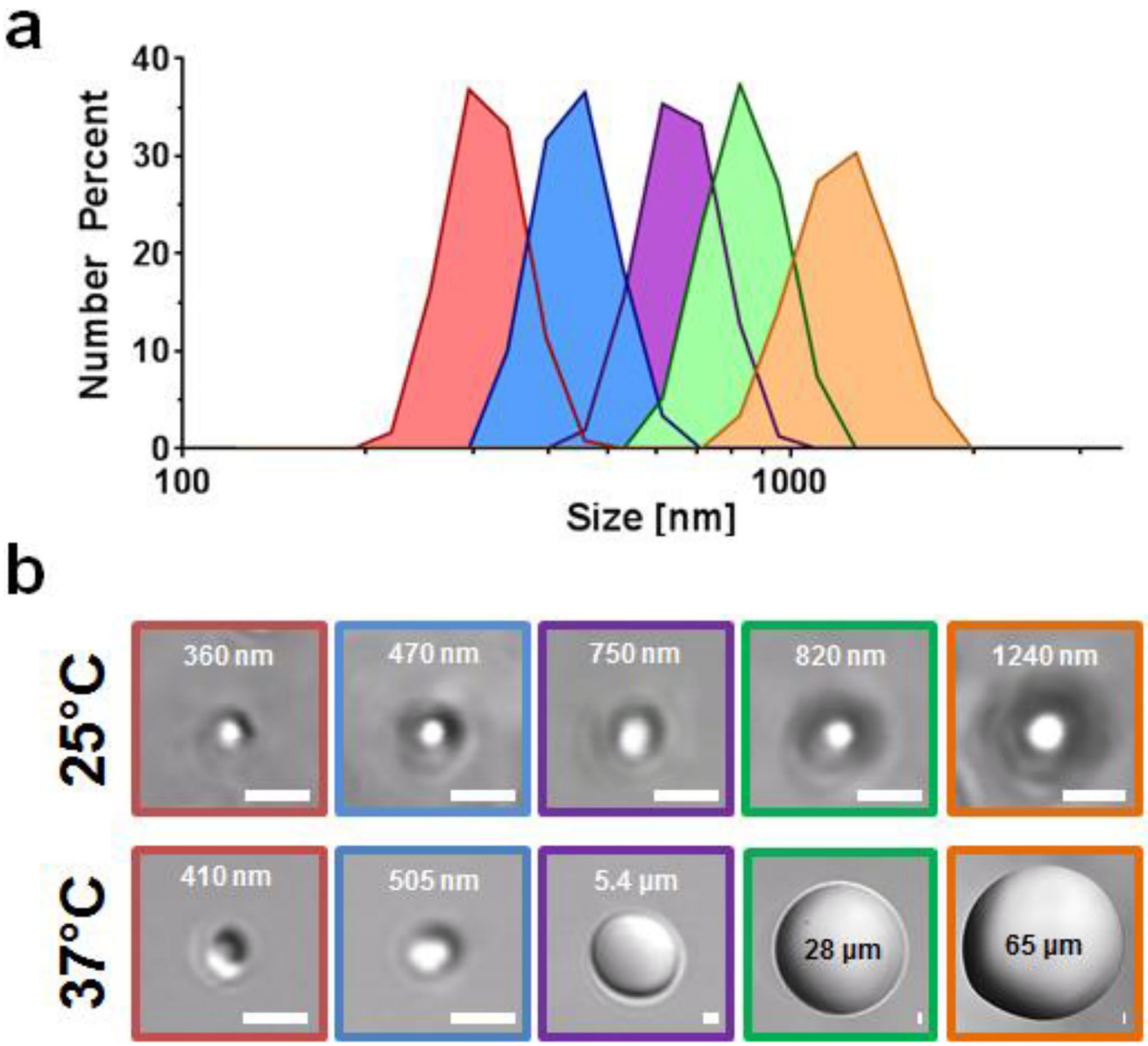


**Figure 2.**

(**a**) Particle size measurement of nano-peptisomes formulated under various peptide and PFP ratios, where each colour represents different formulations (Table 1). (**b**) DIC microscopy images of nano-peptisomes at both room (25°C) and physiologic temperature (37°C); scale bar = 1 µm.

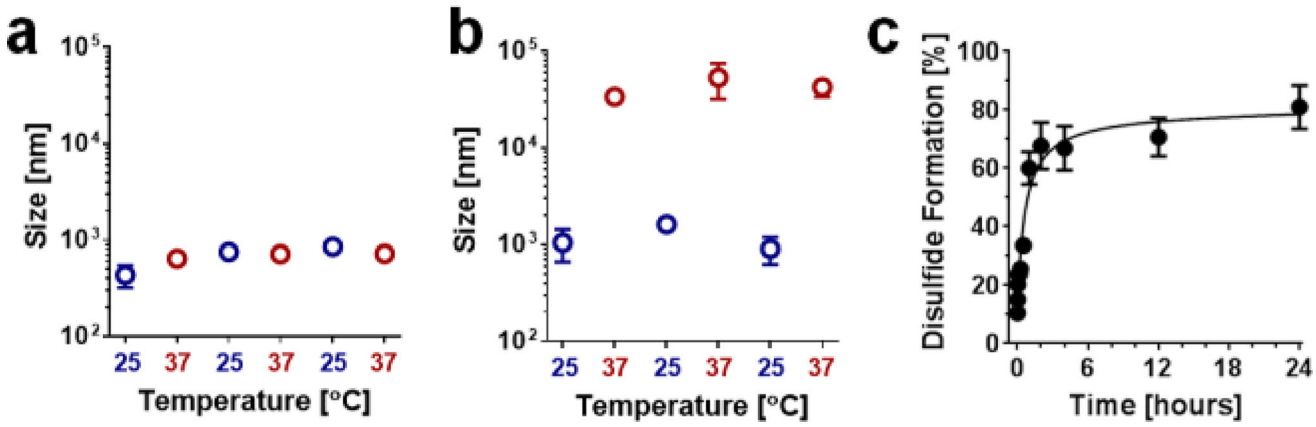


**Figure 3.**

Stability and cross-linking of nano-peptisomes. Change in particle size of (a) formulation #5 and (b) formulation #1 when subjected to repeated thermal cycling. (c) Percentage of disulfide cross-linking as a function of time following nano-peptisome assembly (formulation #5).

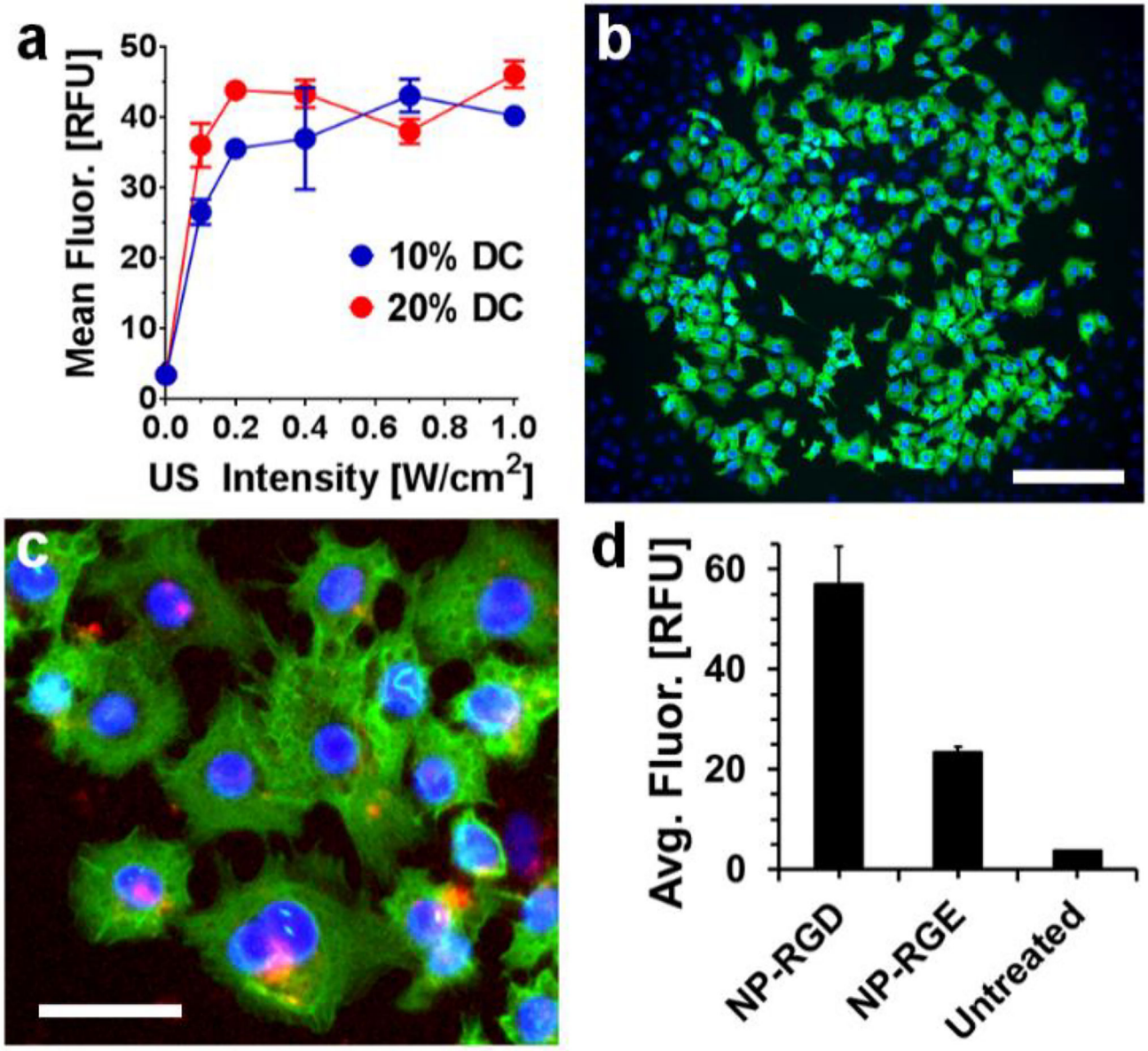


**Figure 4.**

Cytoplasmic delivery of membrane-impermeable phalloidin into cells following US-triggered rupture of nano-peptisomes. (a) Mean intracellular fluorescence (in relative fluorescence units; RFU) of A549 cells following delivery of labelled phalloidin from nano-peptisomes at varying US intensity and duty cycle (DC). (b) Live-cell image showing delivery of phalloidin (green) from nano-peptisomes, spatially resolved to a circular area of the A549 cell monolayer subjected to US. Cell nuclei are stained blue, scale bar = 200 μm. (c) Live A549 cells stained with the endosomal marker transferrin (red) following nano-peptisome mediated delivery of labelled phalloidin. Scale bar = 80 μm. (d) Average intracellular fluorescence of A549 cells upon delivery of labelled phalloidin from nano-

peptisomes (NP) containing the RGD targeting motif, or the non-targeted control sequence RGE

**Table 1**

Physicochemical properties of nano-peptisome formulations

| Formulation | Peptide Conc. [mg/mL] | PFP [vol %] | Droplet size [nm] | | Δ[b] | ζ[c] [mV] |
|---|---|---|---|---|---|---|
| | | | 25°C | 37°C | | |
| 1 | 1.00 | 2 | $1.2 \times 10^3$ | $43 \times 10^3$ | 36.5 | 3.5 ± 0.2 |
| 2 | 1.00 | 1 | 863 ± 98 | $23 \times 10^3$ | 26.7 | 0.1 ± 0.2 |
| 3 | 0.75 | 2 | 739 ± 56 | $7.5 \times 10^3$ | 10.1 | 6.8 ± 0.5 |
| 4[a] | 0.75 | 1 | 469 ± 24 | 482 ± 34 | 1.0 | 8.0 ± 0.4 |
| 5 | 0.50 | 2 | 453 ± 29 | 528 ± 24 | 1.3 | 8.2 ± 0.4 |
| 6[a] | 0.25 | 2 | 448 ± 27 | 458 ± 23 | 1.0 | 4.6 ± 0.2 |
| 7 | 0.50 | 1 | 301 ± 14 | 390 ± 12 | 1.3 | 12.4 ± 0.4 |

[a]Formulations 4 and 6 are not colour coded as they are not shown in Fig. 2a due to their similar size to formulation 5.

[b]folds change in particle size at 37°C versus 25°C.

[c]zeta potential

*Angew Chem Int Ed Engl*. Author manuscript; available in PMC 2018 September 11.